RESEARCH ARTICLE

Tribological behavior of ammonium-based protic ionic liquid as lubricant additive

Hong GUO, Patricia IGLESIAS[*]

Mechanical Engineering Department, Rochester Institute of Technology, New York 14623-5603, USA

© The author(s) 2020.

Abstract: In this study, the tribological behavior of an ammonium-based protic ionic liquid (PIL) as an additive in a base mineral oil (MO) is investigated on a steel–steel contact at room temperature and 100 °C. Tri-[bis(2-hydroxyethylammonium)] citrate (DCi) was synthesized in a simple and low-cost way, and the ionic structure of DCi was confirmed by proton nuclear magnetic resonance (^{1}H NMR). The stability measurement of 1 wt% DCi to a MO was investigated, and the lubricating ability and anti-wear properties of DCi as an additive in MO were also examined using a custom-designed reciprocating ball-on-flat tribometer. Optical microscope and profilometry were used to obtain the worn morphology of the steel disks. Scanning electron microscopy (SEM) and energy dispersive X-ray spectroscopy (EDS) were carried out to investigate the wear mechanism and to analyze the surface interactions between the rubbing components. When 1 wt% DCi is added into the base MO, frictional performance is improved at both temperatures studied with a friction reduction of 29.0% and 35.5%, respectively. Moreover, the addition of 1 wt% DCi to MO reduced the wear volume 59.4% compared to the use of MO. An oxygen-richened tribolayer is confirmed by EDS on the disk surface when DCi was used as additive under 100 °C.

Keywords: protic ionic liquid (PIL); tri-[bis(2-hydroxyethylammonium)] citrate (DCi); steel–steel; friction; wear

1 Introduction

It is estimated that the energy consumption from tribological contacts accounts for 23% which is around 119 EJ of the world's total energy consumption [1]. In order to reduce the energy losses and increase the energy efficiency of mechanical systems, one approach is to add additives, such as friction modifier additives or anti-wear additives, to the lubricant to obtain improved tribological performance [2]. Ionic liquids (ILs) have attracted attention of the research community as lubricants or lubricant additives since they been explored for lubrication in 2001 [3]. ILs are synthetic salts that consist of cations and anions with melting point below 100 °C or even lower. The most commonly used cations of ILs are ammonium [4, 5], imidazolium [6], pyridinium [7], or phosphonium [8, 9], where the

anions could be either organic or inorganic [10]. ILs have a number of unique properties which make them outperform conventional lubricants or lubricant additives, such as high temperature stability, low flammability, negligible volatility as well as high thermal conductivity [3, 11, 12]. Oil-miscible ILs are explored and reported with promising anti-wear properties in early 2012 [13, 14], and since then, ILs used as lubricant additives have become a new topic.

Aprotic ionic liquids (APILs) are a subset of ILs, and have been widely studied for more than a decade and proved to have the potential to be lubricant and lubricant additives [15–19]. However, most of the APILs contain halogen elements such as fluorine or chlorine, which can easily form hydrofluoric or hydrochloric acid when exposed to the moisture atmosphere, and then corrode the metal workpieces. APILs are also

very expensive because of their complicated synthesis route [20]. Protic ionic liquids (PILs), which are another subset of ILs, can be easily obtained by combination of a Brønsted acid and a Brønsted base. These PILs possess a wide range of properties, such as high viscosity, high thermal and electronic conductivity, non-flammability, and low toxicity [21]. These properties make PILs suitable in many areas such as catalyst [22, 23], nanostructured materials [24], and electrochemistry [25]. Ethylammonium nitrate [$(C_2H_5NH_3)NO_3$] is found to be the first PIL at room-temperature and reported by Walden in 1914 [26]. PILs can be tailored by changing cation structures, anion structures or both to satisfy specific requirements [22, 27–29]. Due to the easy synthetic route, low cost and toxicity, PILs can be a suitable alternative to APILs in lubrication.

When lubricants are used in the automotive industry, they are not only being used to protect the engine but also should be formulated to minimize the impact on the exhaust after treatment devices, such as catalytic converters or diesel particulate filters [30]. It is found that phosphorus oxides, sulfur oxides, and ash will reduce the effective life of exhaust catalysts, leading to the limitation of the level of phosphorus and sulfur in engine oils [31]. The development of more environmentally-friendly ILs that are free from halogens, sulfurs, and phosphorus is needed to satisfy the restrictive regulations [32].

In this work, a protic ammonium cation and carboxylate anion, with only carbons, hydrogens, nitrogen, and oxygens, will be used as a new PIL. The lubricating ability and anti-wear property of this ammonium-based PIL as additive to a commercially available mineral oil (MO) in steel–steel contact mode will be investigated using a ball-on-flat reciprocating tribometer.

2 Materials and methods

The base oil used in this study is a MO provided by Repsol (Spain), and its properties are summarized in Table 1. Diethanolamine (≥ 98.0%) and citric acid (≥ 99.5%) were purchased from Sigma Aldrich (USA). The PIL, tri-[bis(2-hydroxyethylammonium)] citrate (DCi), was synthesized in our laboratory through the
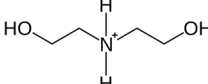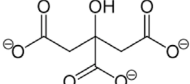
following process [33]: 0.6 mol diethanolamine was dissolved in ethanol (100 ml) to form a liquid solution, and shifted to a 500 ml three neck round bottom flask. A magnetic stirrer was placed under the flask, a reflux condenser and a pressure equalizing additional funnel were connected to the flask in turn. 0.2 ml citric acid was dissolved in 100 ml of ethanol, and the mixture was shifted to the pressure equalizing additional funnel and dropwise added to the flask under the argon atmosphere in 2 hours. After the reaction was completed, the upper suspended ethanol was removed, and the final mixture was heated in a water bath at 78 °C to evaporate the remaining ethanol under argon atmosphere. In the end, the consequent viscous liquid was dried under a vacuum line for 7 hours. The molecular structure of the product was analyzed by proton nuclear magnetic resonance (^{1}H NMR) using a Bruker Ultrashield 300 MHz spectrometer, with DMSO-d6 as solvent and TMS as internal standard. The molecular structure and empirical formula of DCi are summarized in Table 2.

In this research, DCi was added in 1 wt% to MO to form a homogeneous mixture at room temperature through magnetic stirring for 6 hours, and ultra-sonicating for 0.5 hour. In addition, to study the stability of 1 wt% DCi in MO, the mixtures were centrifuged at 6,500 rpm for 10 min, and then observed the appearance of the mixture after 24, 168, and 720 hours. Thermogravimetric analysis (TGA) of MO and DCi were conducted with a TA Instrument Q500 from ambient temperature to 600 °C at a heating rate of 10 °C/min and a flow rate of 20 mL/min in air. Dynamic viscosity measurements of MO, pure DCi,

Table 1 Properties of MO used in this study.

Density at 15 °C (g/mL)	Kinematic viscosity (mm²/s)		Viscosity index	Flash point (°C)	Pour point (°C)
	40 °C	100 °C			
0.8668	45.91	6.676	97	234	−12

Table 2 Molecular structure and empirical formula of DCi.

Molecular structure		Empirical formula
Cation	Anion	
		$C_{18}H_{41}O_{13}N_3$

and 1 wt% DCi+MO were carried out by a Brookfield DV2T viscometer with a thermosel system.

Tribological tests were conducted in a reciprocating ball-on-flat tribometer (Fig. 1(a)), with a heater to run tests at room temperature and 100 °C, respectively. In the reciprocating tests, AISI 52100 steel disks (hardness ≈ 22.3 HRC and Ra ≈ 0.008 μm) slid against AISI 52100 steel balls (hardness ≈ 58 HRC and Ra ≈ 0.53 μm) with diameter of 1.5 mm. The tribotests were carried out under a normal load of 2 N, which corresponds to a mean Hertz contact pressure of 1.34 GPa and a maximum Hertz contact pressure of 2.02 GPa. The sliding speed for each test was set to 0.05 m/s with frequency of 5 Hz, stroke length of 5 mm, and sliding distance of 200 m.

At least three tests were performed under the same conditions for each lubricant at room temperature and 100 °C. Prior to each test, 1 mL of lubricant was added on the disk surface and no additional lubricant was added during the testing process. Once completing each trial, the disk was placed in an ultrasonic cleaner with isopropyl alcohol (99.5%) until the sample was cleaned completely, and then dried in air. Friction coefficients were recorded over time and calculated as average of each running. After tests, an Olympus BH-2 optical microscope was used to measure the width of wear tracks and at least 15 measurements were taken along each wear track. The wear volume was calculated according to Eq. (1) [34]. A Nanovea ST 400 profilometer was also used to study the 3-dimensional (3D) images of the wear tracks. A Tescan Mira3 scanning electron microscope (SEM) and energy disper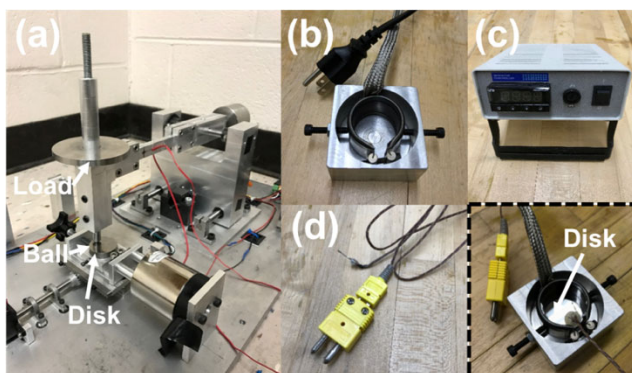sive spectrometer (EDS) were used to analyze the wear mechanism and surface interaction between the steel disks and steel balls.

$$V_f = L_s \left[R_f^2 \arcsin\left(\frac{W}{2R_f}\right) - \frac{W}{2}(R_f - h_f) \right] + \frac{\pi}{3}h_f^2(3R_f - h_f)$$

$$h_f = R_f - \sqrt{R_f^2 - \frac{W^2}{4}} \quad (1)$$

where V_f is wear volume, L_s is stroke length, R_f is radius of the ball, W is width of the wear scar, and h_f is wear depth.

3 Results and discussion

3.1 NMR and stability tests

NMR spectrum was carried out to analyze and to confirm the ionic structure of DCi and the results are shown in Fig. 2. The abbreviations used below are to designate the multiplicities: s = singlet, and t = triplet. δ = 4.46 (s, 13H, NH$_2$, OH) corresponds to hydrogens of –OH and –NH from the IL cation. When δ = 3.55–3.60 (t, 12H, CH$_2$, CH$_2$, CH$_2$, CH$_2$, CH$_2$, CH$_2$), the peaks are related to the hydrogens of –CH$_2$ also in cations. When δ = 2.77–2.85 (t, 12 H, N–CH2, N–CH$_2$, N–CH$_2$, N–CH$_2$, N–CH$_2$, N–CH$_2$), the peaks correspond to the hydrogens of –CH$_2$, whose carbon is connected with the nitrogen from cations of DCi. The peak for δ = 2.5 is the characteristic peak of hydrogen in DMSO-d6. When δ = 2.33–2.4 (s, 4H, C=O–CH$_2$), the peaks are related to the hydrogen in C=O–CH$_2$ of anions. This spectrum confirms the ionic structure of DCi.

Figure 3 shows the stability samples of 1 wt% DCi in MO. From the Fig. 3, there is no visual deposit on the bottom of each centrifugal capsule after observation for 24, 168, and 720 hours. These results confirm the good stability of 1 wt% DCi in MO.
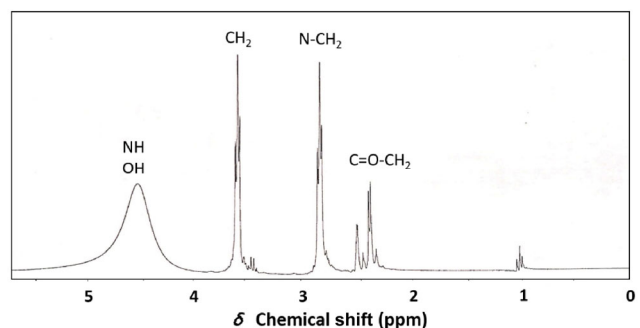

Fig. 1 Images of (a) reciprocating ball-on-flat tribometer and (b–d) experimental kit used for tribotests in high temperature: (b) sample holder, (c) temperature controller, and (d) thermal couple.
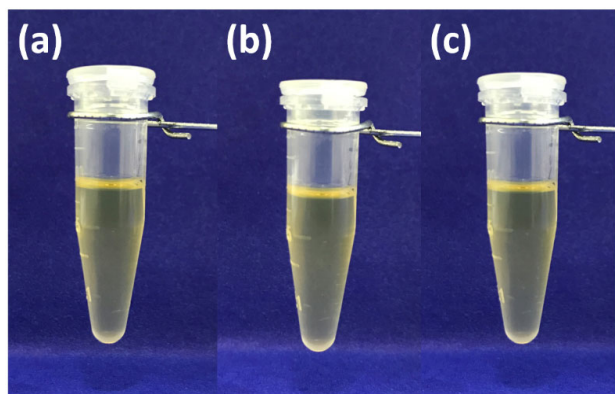

Fig. 2 NMR spectrum of DCi.

Fig. 3 Proof of stability of 1 wt% DCi in MO after (a) 24, (b) 168, and (c) 720 h.

3.2 Thermal stability and viscosity of the lubricants

The thermal stability of MO, pure DCi, and the mixture 1 wt% DCi+MO were examined by thermogravimetric analysis (TGA) and the results are summarized in Table 3 and Fig. 4. MO has higher thermal stability than pure DCi, with onset decomposition temperatures of 291.2 and 191.2 °C, respectively. When 1 wt% DCi is added into the base MO, the mixture exhibits slightly higher thermal stability than MO, with an onset temperature of 300.4 °C.

Viscosity is one of the most important physical properties of a lubricant. Viscosity tests were performed with MO, pure DCi, and the mixture of 1 wt% DCi+ MO. The average dynamic viscosity as a function of

Table 3 Thermal stability of MO, DCi, and 1 wt% DCi+MO.

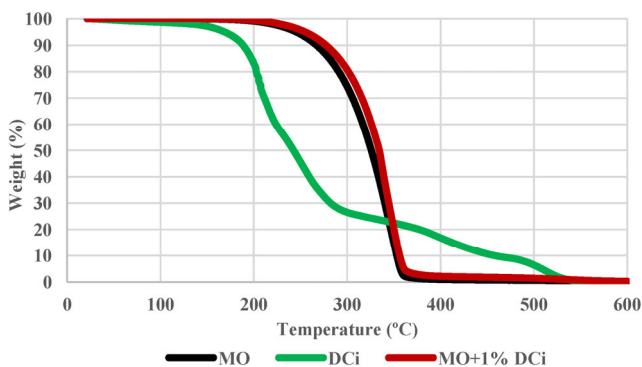| Lubricant	Onset temperature (°C)
MO	291.2
DCi	191.2
1 wt% DCi+MO	300.4

Fig. 4 Experimental TGA for MO, DCi, and 1 wt% DCi+MO.

temperature of these lubricants are shown in Fig. 5 and Table 4. It is well known that ion–ion interactions and hydrogen bonding between molecules will impact the lubricant viscosity. In general, greater chemical interactions lead to higher viscosity [29]. Pure DCi shows a higher viscosity than MO at room temperature due to the hydrogen bondings between cations and anions. When 1 wt% DCi was added into MO, the viscosity of the mixture is increased slightly compared to neat MO.

3.3 Tribological properties

The lubricating ability of MO and 1 wt% DCi+MO at room temperature and 100 °C under reciprocating steel–steel contact mode were studied using a ball-on-flat tribometer. Figure 6 shows the average value of the friction coefficient of the lubricants at room temperature and 100 °C. Adding 1 wt% DCi to the MO reduced the friction coefficient at both temperatures. Increasing the temperature, increased the friction coefficient when the steel sliding surfaces are lubricated
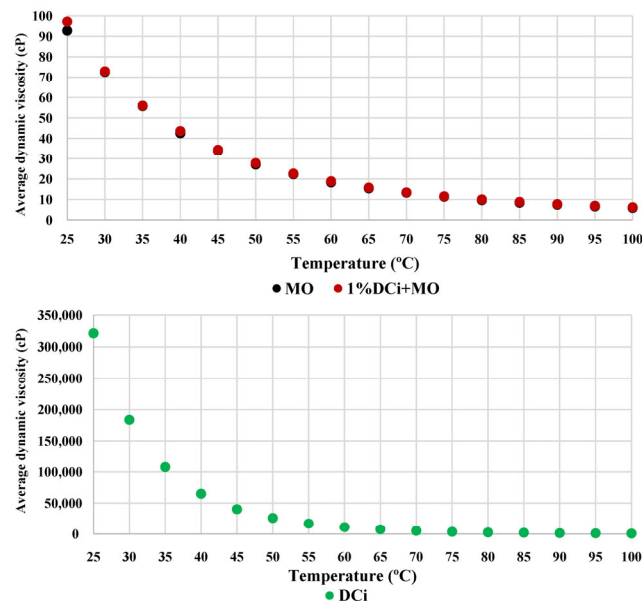

Fig. 5 Viscosity of MO, pure DCi, and mixture 1 wt% DCi+MO.

Table 4 Viscosity of MO, DCi, and 1 wt% DCi+MO.

Lubricant	Dynamic viscosity (cP)		
	25 ℃	40 ℃	100 ℃
MO	92.78	42.54	5.90
DCi	321,691.43	65,097.14	941.21
1 wt% DCi+MO	97.17	43.58	6.22
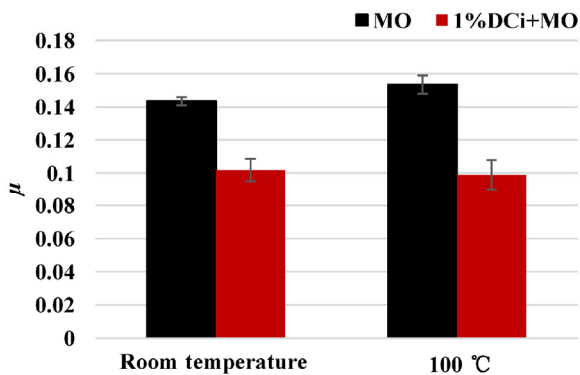
Fig. 6 Average friction coefficients as a function of temperature.

Fig. 8 Optical images of worn balls after lubricated with (a) MO at room temperature, (b) MO at 100 ℃, (c) 1 wt% DCi+MO at room temperature, and (d) 1 wt% DCi+MO at 100 ℃.

with MO, however when 1 wt% DCi+MO is used as lubricant, the friction coefficient remains constant. A maximum friction reduction of 35.5% is obtained when the mixture was used as lubricant compared with neat MO at 100 °C.

Figure 7 summarizes the wear volumes of the sliding disks after tests lubricated with MO and 1 wt% DCi+MO at room temperature and 100 °C. At room temperature, the presence of DCi in the lubricant slightly increased the wear volume of the steel disks. However, at the higher temperature studied, the disk lubricated with 1 wt% DCi+MO led to a less wear loss with a wear reduction of 59.4% with respect to the MO. These results confirm the good lubricating ability of 1 wt% DCi+MO at high temperature.

The optical micrographs of the worn balls lubricated with MO and 1 wt% DCi+MO at room temperature and 100 °C are shown in Fig. 8. The wear scars (Figs. 8(b) and 8(d)) obtained at high temperature are larger than the ones formed at room temperature (Figs. 8(a) and 8(c)). There is no significant difference between the wear scars obtained after tests run at room temperature (Figs. 8(a) and 8(c)). However, adding DCi to MO reduced the size of the steel ball
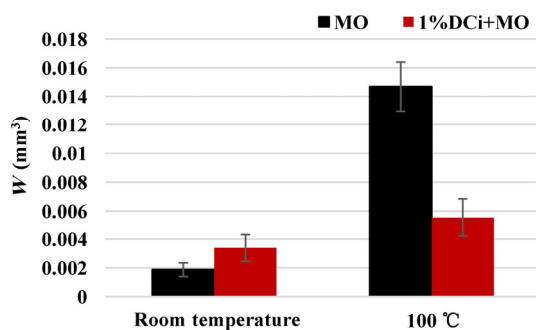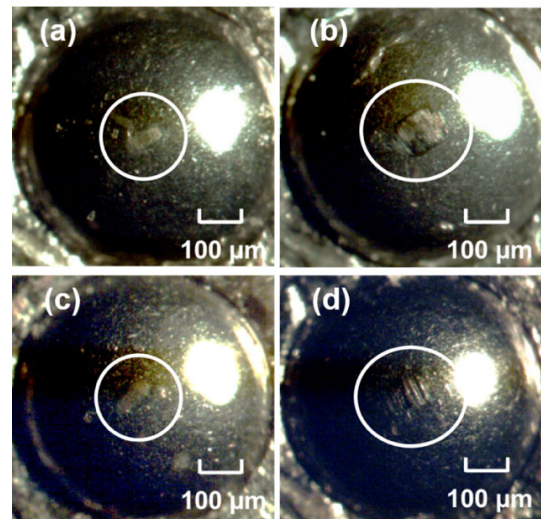
wear track (Figs. 8(b) and 8(d)) at high temperature, confirming that the presence of DCi in the lubricant improves the wear prevention of the sliding disks as well as the pairing components.

Figure 9 shows the optical images of the worn surfaces of the steel disks after frictional tests lubricated with MO and 1 wt% DCi+MO. As expected, increasing the temperature increased the wear volume on the steel disks for both lubricants. However, when DCi was used as additive at 100 °C, a more uniform and narrower wear track is observed compared to that obtained after a test lubricated with neat MO. For both lubricants, clear abrasive marks parallel to the sliding direction are observed on steel surfaces at 100 °C. In addition to the plowing effect, plastic deformation and pits can be observed on the worn steel surface when lubricated with MO at 100 °C.

In order to verify the wear depth variations of the steel disks when lubricated with MO and 1 wt% DCi+MO under room temperature and 100 °C, Nanovea ST 400 profilometer was used to obtain the 3D images (Fig. 10) and 2D images (Fig. 11) of the wear tracks on the steel disks. In Figs. 10 and 11, the depth of the wear track increases as the temperature goes up for both lubricants. Comparing the images in Figs. 10(a and c) and 11(a and c), wear tracks after a test lubricated with MO are narrower and shallower than those obtained after a test lubricanted with 1 wt% DCi+MO at room temperature. When the
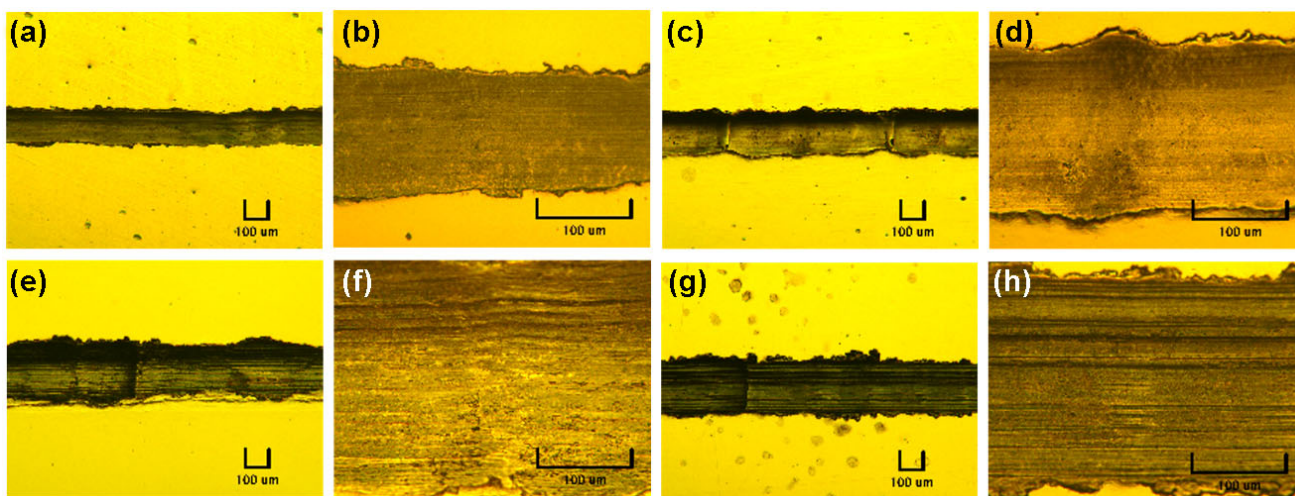

Fig. 7 Wear volume of steel disks as a function of temperature.

Fig. 9 Optical images of wear tracks on the steel disks after sliding 200 m and lubricated with (a and b) MO at room temperature, (c and d) 1 wt% DCi+MO at room temperature, (e and f) MO at 100 ºC, (g and h) 1 wt% DCi+MO at 100 ºC. Left images display with 50× zoom and right images display with 200× zoom.
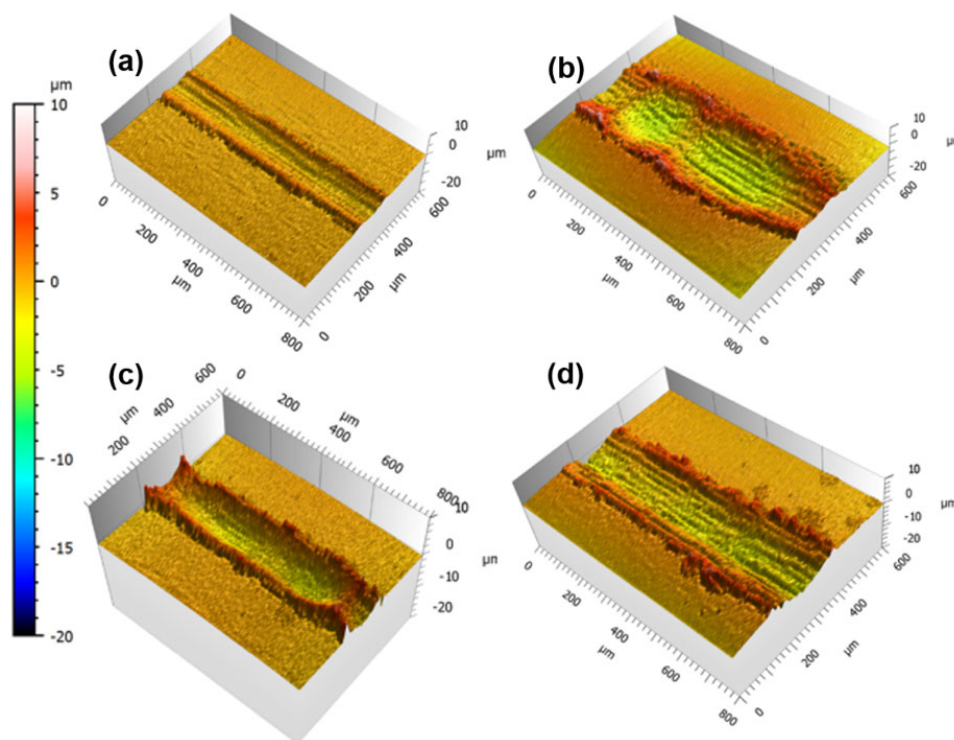

Fig. 10 3D profilometer images of wear tracks on the steel disks after lubricated with (a) MO at room temperature, (b) MO at 100 ºC, (c) 1 wt% DCi+MO at room temperature, and (d) 1 wt% DCi+MO at 100 ºC.

temperature increases to 100 °C, the mixture outperforms MO in preventing wear on the steel disks. In Figs. 10(b) and 11(b), both the depth and width of the wear tracks are larger than the one in Figs. 10(d) and 11(d).

SEM and EDS were used to analyze the wear mechanism and surface interactions between rubbing components. The SEM micrographs of wear tacks on the steel disks after lubricated with MO and 1 wt% DCi+MO at room temperature and 100 °C are shown in Fig. 12. The abrasive marks can be seen in all the images, but particularly at high temperature for both
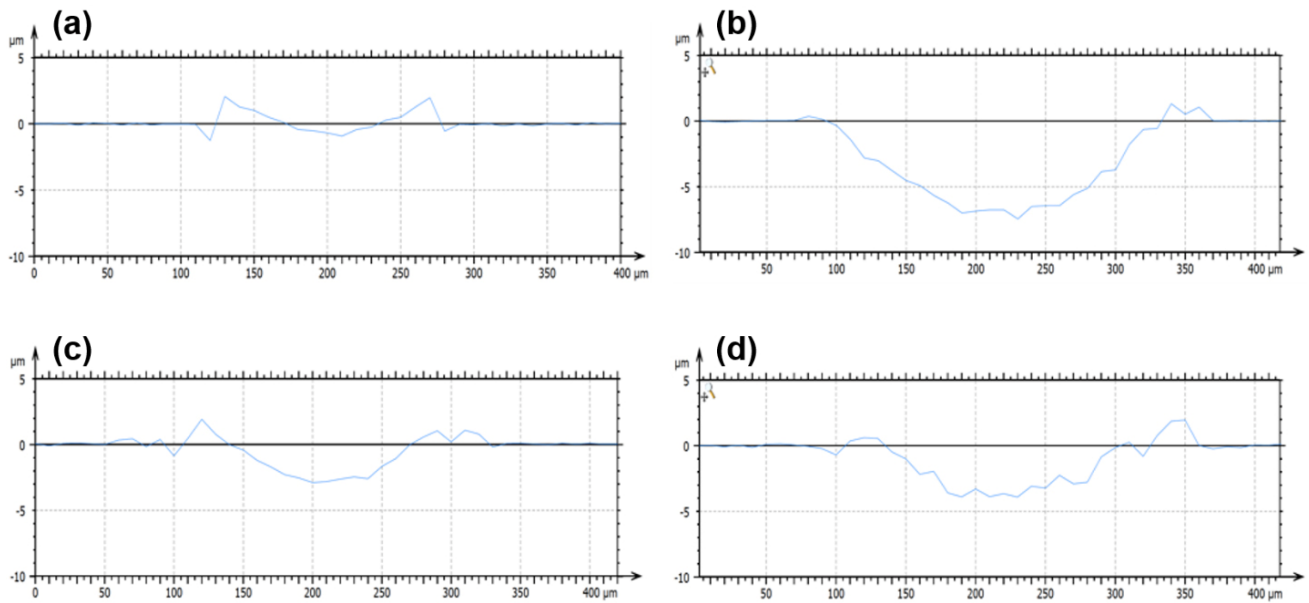
Fig. 11 2D profiles of wear tracks on the steel disks after lubricated with (a) MO at room temperature, (b) MO at 100 ºC, (c) 1 wt% DCi+MO at room temperature, and (d) 1 wt% DCi+MO at 100 ºC.
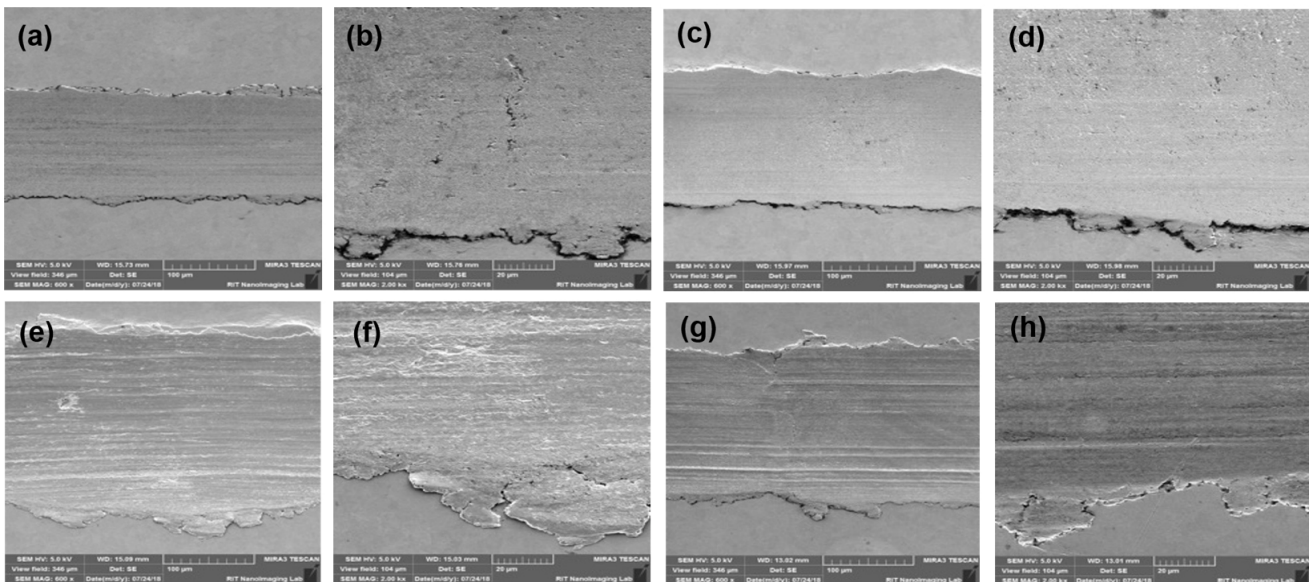

Fig. 12 SEM micrographs of wear tracks on the steel disks after a sliding distance of 200 m and lubricated with (a and b) MO at room temperature, (c and d) 1 wt% DCi+MO at room temperature, (e and f) MO at 100 ºC, (g and h) 1 wt% DCi+MO at 100 ºC. Left images display with 600× zoom and right images display with 2,000× zoom.

lubricants (Figs. 12(e)–12(h)). An important component of plastic deformation with material accumulated at the borders of the wear tracks is also seem at both temperatures.

In order to understand the lubricating mechanism of DCi as lubricant additive at high temperature, EDS analysis was carried out inside and outside of the wear tracks after a test lubricated with MO and 1 wt% DCi+MO at 100 °C, and results are shown in Figs. 13(a) and 13(b). Both worn surfaces show higher amount of oxygen and a slightly higher carbon inside the wear track compared to the outside. However, according to the spectra, the amount of oxygen on the worn surface is higher when the sample surface was lubricated with 1 wt% DCi+MO, where the oxygen is homogeneously distributed inside of the wear track
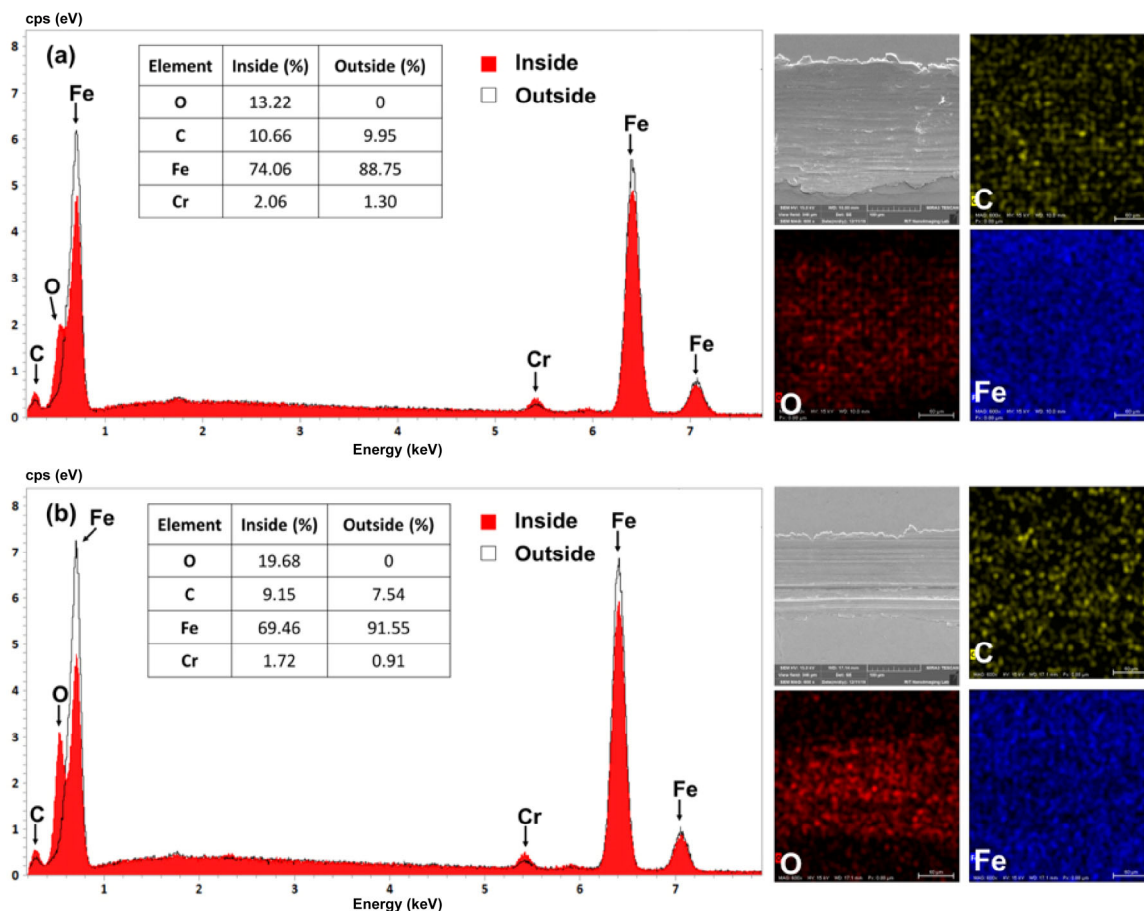
Fig. 13 EDS spectrum inside and outside the wear track and element mapping after lubricated with (a) MO at 100 ºC and (b) 1 wt% DCi+MO at 100 ºC.

(see the element mapping in Fig. 13(b)). This oxygen-richened tribolayer may be responsible for the good lubricating behavior when 1 wt% DCi is present in the lubricating system [29, 35].

4   Conclusions

The tribological ability of a new synthesized protic ionic liquid tri-[bis(2-hydroxyethylammonium)] citrate (DCi) is studied as additive to a base MO for a steel–steel contact mode at room temperature and 100 °C. When 1 wt% DCi is added into MO, lower friction coefficient at both temperatures are observed compared to MO, with friction reductions of 29.0% at room temperature, and 35.5% at 100 °C. In addition to these promising friction results, 1 wt% DCi+MO also exhibits an excellent anti-wear performance at 100 °C where the wear reduction reaches up to 59.4% compared to MO. Abrasive marks and plastic deformation with

accumulated material along the borders of the wear tracks can be seen from optical and SEM images of the worn surfaces after tests lubricated with MO and 1 wt% DCi+MO. In particular, when 1wt% is added to MO, wear tracks obtained after tests at high temperature are narrower and swallower than those obtained after a test lubricated with MO. From EDS analysis, a carbon and oxygen-richened tribolayer is formed on the surface when DCi was used as additive at 100 °C, that may be responsible for improving the friction and wear performance at this temperature.

References

[1] Holmberg K, Erdemir A. Influence of tribology on global energy consumption, costs and emissions. *Friction* **5**(3): 263–284 (2017)

[2] Spikes H. Friction modifier additives. *Tribol Lett* **60**(1): 5 (2015)

[3] Ye C, Liu W, Chen Y, Yu L. Room-temperature ionic liquids: A novel versatile lubricant. *Chem Commun* **7**(21): 2244–2245 (2001)

[4] Li Z P, Ren T H. Synergistic effects between alkylphosphate-ammonium ionic liquid and alkylphenylborate as lubricant additives in rapeseed oil. *Tribol Int* **109**: 373–381 (2017)

[5] Qu J, Truhan J J, Dai S, Luo H, Blau P J. Ionic liquids with ammonium cations as lubricants or additives. *Tribol Lett* **22**(3): 207–214 (2006)

[6] Cai M R, Liang Y M, Yao M H, Xia Y Q, Zhou F, Liu W M. Imidazolium ionic liquids as antiwear and antioxidant additive in poly(ethylene glycol) for steel/steel contacts. *ACS Appl Mater Interfaces* **2**(3): 870–876 (2010)

[7] Mahrova M, Pagano F, Pejakovic V, Valea A, Kalin M, Igartua A, Tojo E. Pyridinium based dicationic ionic liquids as base lubricants or lubricant additives. *Tribol Int* **82**: 245–254 (2015)

[8] Hernández Battez A, Bartolomé M, Blanco D, Viesca J L, Fernández-González A, González R. Phosphonium cation-based ionic liquids as neat lubricants: Physicochemical and tribological performance. *Tribol Int* **95**: 118–131 (2016)

[9] Guo H, Liu R, Fuentes-Aznar A, Victoria P I. Friction and wear properties of halogen-free and halogen-containing ionic liquids used as neat lubricants, lubricant additives and thin lubricant layers. In *2017 International Design Engineering Technical Conferences and Computers and Information in Engineering Conference*, Cleveland, Ohio, USA, 2017.

[10] Zhou Y, Qu J. Ionic liquids as lubricant additives: A review. *ACS Appl Mater Interfaces* **9**(4): 3209–3222 (2017)

[11] Arcifa A, Rossi A, Espinosa-Marzal R M, Spencer N D. Influence of environmental humidity on the wear and friction of a silica/silicon tribopair lubricated with a hydrophilic ionic liquid. *ACS Appl Mater Interfaces* **8**(5): 2961–2973 (2016)

[12] Matczak L, Johanning C, Gil E, Guo H, Smith T W, Schertzer M, Iglesias P. Effect of cation nature on the lubricating and physicochemical properties of three ionic liquids. *Tribiol Int* **124**: 23–33 (2018)

[13] Mistry K, Fox M F, Priest M. Lubrication of an electroplated nickel matrix silicon carbide coated eutectic aluminium-silicon alloy automotive cylinder bore with an ionic liquid as a lubricant additive. *Proc Inst Mech Eng Part J J Eng Tribol* **223**(3): 563–569 (2009)

[14] Jiménez A E, Bermúdez M D. Short alkyl chain imidazolium ionic liquid additives in lubrication of three aluminium alloys with synthetic ester oil. *Tribol-Mater Surf Interfaces* **6**(3): 109–115 (2012)

[15] Pejaković V, Kronberger M, Mahrova M, Vilas M, Tojo E, Kalin M. Pyrrolidinium sulfate and ammonium sulfate ionic liquids as lubricant additives for steel/steel contact lubrication. *Proc Inst Mech Eng Part J J Eng Tribol* **226**(11): 923–932 (2012)

[16] Liu X Q, Zhou F, Liang Y M, Liu W M. Tribological performance of phosphonium based ionic liquids for an aluminum-on-steel system and opinions on lubrication mechanism. *Wear* **261**(10): 1174–1179 (2006)

[17] Yu B, Bansal D G, Qu J, Sun X Q, Luo H M, Dai S, Blau P J, Bunting B G, Mordukhovich G, Smolenski D J. Oil-miscible and non-corrosive phosphonium-based ionic liquids as candidate lubricant additives. *Wear* **289**: 58–64 (2012)

[18] Patel A, Guo H, Iglesias P. Study of the lubricating ability of protic ionic liquid on an aluminum–steel contact. *Lubricants* **6**(3): 66 (2018)

[19] Del Sol I, Gámez A J, Rivero A, Iglesias P. Tribological performance of ionic liquids as additives of water-based cutting fluids. *Wear* **426–427**: 845–852 (2019)

[20] Ratti R. Ionic liquids: Synthesis and applications in catalysis. *Adv Chem* **2014**: 729842 (2014)

[21] Kondo H. Protic ionic liquids with ammonium salts as lubricants for magnetic thin film media. *Tribol Lett* **31**(3): 211–218 (2008)

[22] Duan Z Y, Gu Y L, Zhang J, Zhu L Y, Deng Y Q. Protic pyridinium ionic liquids: Synthesis, acidity determination and their performances for acid catalysis. *J Mol Catal A Chem* **250**(1–2): 163–168 (2006)

[23] Tong X L, Ma Y, Li Y D. An efficient catalytic dehydration of fructose and sucrose to 5-hydroxymethylfurfural with protic ionic liquids. *Carbohydr Res* **345**(12): 1698–1701 (2010)

[24] Hayes R, Imberti S, Warr G G, Atkin R. Effect of cation alkyl chain length and anion type on protic ionic liquid nanostructure. *J Phys Chem C* **118**(25): 13998–14008 (2014)

[25] Shmukler L E, Gruzdev M S, Kudryakova N O, Fadeeva Y A, Kolker A M, Safonova L P. Thermal behavior and electrochemistry of protic ionic liquids based on triethylamine with different acids. *RSC Adv* **6**(111): 109664–109671 (2016)

[26] Walden P. Molecular weights and electrical conductivity of several fused salts. *Bull Acad Imper Sci (St. Petersburg)* **1800**: 405–422 (1914)

[27] Vega M R O, Parise K, Ramos L B, Boff U, Mattedi S, Schaeffer L, Malfatti C F. Protic ionic liquids used as metal-forming green lubricants for aluminum: Effect of anion chain length. *Mater Res* **20**(3): 675–687 (2017)

[28] Espinosa T, Sanes J, Jiménez A E, Bermúdez M D. Protic ammonium carboxylate ionic liquid lubricants of OFHC copper. *Wear* **303**(1–2): 495–509 (2013)

[29] Greaves T L, Drummond C J. Protic ionic liquids: Properties and applications. *Chem Rev* **108**(1): 206–237 (2008)

[30] Canter N. Special Report: Additive challenges in meeting new automotive engine specifications. *Tribol Lubr Technol* **62**(9): 10–19 (2006)

[31] Spikes H. The history and mechanisms of ZDDP. *Tribol Lett* **17**(3): 469–489 (2004)

[32] Espinosa T, Jiménez M, Sanes J, Jiménez A E, Iglesias M, Bermúdez M D. Ultra-low friction with a protic ionic liquid boundary film at the water-lubricated sapphire-stainless steel interface. *Tribol Lett* **53**(1): 1–9 (2014)

[33] Iglesias M, Gonzalez-Olmos R, Cota I, Medina F. Brønsted ionic liquids: Study of physico-chemical properties and catalytic activity in aldol condensations. *Chem Eng J* **162**(2): 802–808 (2010)

[34] Qu J, Truhan J J. An efficient method for accurately determining wear volumes of sliders with non-flat wear scars and compound curvatures. *Wear* **261**(7–8): 848–855 (2006)

[35] Cigno E, Magagnoli C, Pierce M S, Iglesias P. Lubricating ability of two phosphonium-based ionic liquids as additives of a bio-oil for use in wind turbines gearboxes. *Wear* **376–377**: 756–765 (2017)
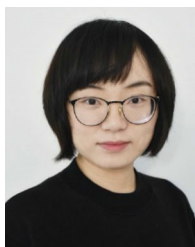
Hong GUO. She received her B.E. degree in metal material in 2010 from Zhengzhou University, Zhengzhou, China. Then she earned her M.S. degree in functional metal materials from Jinan University, Guangzhou, China, in 2014. Now she is a Ph.D. candidate in the Tribology Laboratory of the Kate Gleason College of Engineering at Rochester Institute of Technology. Her current research focuses on investigation of environmentally friendly ionic liquids as lubricants or lubricant additives, sliding and rolling friction of materials, and lubrication and wear mechanism of different tribology systems.

Patricia IGLESIAS. She earned her Ph.D. in mechanical engineering with focus on tribology from the Polytechnic University of Cartagena (Spain). Dr. Iglesias also worked as a post-doctoral researcher in the Center for Materials Processing and Tribology at Purdue University. Currently, she is an associate professor and the director of the Tribology Laboratory in the Kate Gleason College of Engineering at the Rochester Institute of Technology. Her research focuses on wear and friction of materials, ionic liquids as lubricants and additives of lubricants, bio-lubricants, nanostructured materials, and textured surfaces. Dr. Iglesias has extensive experience working on tribology and has published 35 peer-reviewed articles and more than 38 conference proceedings in the area.